The Aurora kinase inhibitor SNS-314 shows broad therapeutic potential with chemotherapeutics and synergy with microtubule-targeted agents in a colon carcinoma model

Erica C. VanderPorten,[1] Pietro Taverna,[2] Jennifer N. Hogan,[2] Marcus D. Ballinger,[1] W. Michael Flanagan,[1] and Raymond V. Fucini[1]

[1]Biology and [2]Pharmacology, Sunesis Pharmaceuticals, Inc., South San Francisco, California

Abstract

Aurora kinases play key roles in regulating centrosome maturation, mitotic spindle formation, and cytokinesis during cell division, and are considered promising drug targets due to their frequent overexpression in a variety of human cancers. SNS-314 is a selective and potent pan Aurora inhibitor currently in a dose escalation phase 1 clinical trial for the treatment of patients with advanced solid tumors. Here, we report the antiproliferative effects of SNS-314 in combination with common chemotherapeutics in cell culture and xenograft models. The HCT116 colorectal carcinoma cell line, with intact or depleted p53 protein levels, was treated with SNS-314 and a cytotoxic chemotherapeutic from a panel comprised of gemcitabine, 5-fluorouracil (5-FU), carboplatin, daunomycin, SN-38 (the active metabolite of irinotecan), docetaxel, and vincristine. Combinations were administered under either concurrent or sequential schedules. SNS-314 has predominantly additive effects when administered concurrently with commonly used anticancer agents. Sequential administration of SNS-314 with chemotherapeutic compounds showed additive antiproliferative effects with carboplatin, gemcitabine, 5-FU, daunomycin, and SN-38, and synergy was observed in combination with gemcitabine, docetaxel, or vincristine. The most profound antiproliferative effects were observed with sequential administration of SNS-314 followed by docetaxel or vincristine. *In vivo*, SNS-314 potentiated the antitumor activity of docetaxel in xenografts. Both the *in vitro* synergies observed between SNS-314 and agents that target the mitotic spindle and the potentiation seen with docetaxel *in vivo* are consistent with a mechanism of action in which Aurora inhibition bypasses the mitotic spindle assembly checkpoint and prevents cytokinesis, augmenting subsequent spindle toxin–mediated mitotic catastrophe and cell death. [Mol Cancer Ther 2009;8(4):930–9]

Introduction

Aurora kinases (isoforms A, B, and C) constitute a family of serine-threonine kinases that play fundamental roles in regulating cell division (1–4). Aurora-A localizes to the centrosomes and functions in centrosome regulation and mitotic spindle formation (5, 6). Aurora-B is characterized as a subunit of the chromosomal passenger protein complex that functions to insure chromosomal segregation and cytokinesis (7, 8). Aurora-C has been identified as a chromosomal passenger protein with similar localization to Aurora-B during mitosis (9). Although the role of Aurora-C is less well established, the enzyme is highly expressed in the testes in which it seems to play a central role in spermatogenesis (3, 9). Elevated Aurora-A expression has been detected in a high percentage of colon, breast, ovarian, gastric, and pancreatic tumors, and Aurora-B and Aurora-C are also expressed at high levels in both primary tumors and cell lines (6, 10–20). Given the central role of all three Aurora kinases in mitotic regulation and the association between their overexpression and tumorigenesis, they are being evaluated as potential targets in cancer therapy (4, 15, 21–24).

We have previously described SNS-314, a selective and potent pan-Aurora inhibitor currently in phase 1 clinical trials for the treatment of patients with advanced solid tumors (25, 26). The cellular phenotypes of most pan-Aurora inhibitors (including SNS-314) are dominated by the effects resulting from Aurora-B inhibition, which leads to multiple defects in mitosis, including aberrant centrosome duplication, disruption of the spindle checkpoint, and inhibition of cytokinesis, which in turn lead to endoreduplication, polyploidy, and cytostasis or cell death (22). Preclinical studies have shown that SNS-314 has broad activity *in vitro* against multiple human cancer cell lines and exhibits significant *in vivo* activity against a wide range of tumor xenograft models. SNS-314 is able to inhibit tumor growth in an intermittent schedule, differentiating it from many other Aurora inhibitors and suggesting the potential for combinations with other targeted or cytotoxic anticancer therapeutics.

Along with SNS-314, a number of small-molecule Aurora inhibitors including MK-0457 (VX-680), AZD1152, PHA-739358, MLN8054, R763, AT9283, and CYC116 are currently undergoing phase 1 or phase 2 clinical evaluations, and the preliminary results have thus far shown disease stabilization as the major clinical response (reviewed in ref. 22), thus it is becoming compelling to evaluate the therapeutic activity of

Received 8/12/08; revised 12/17/08; accepted 12/20/08.

The costs of publication of this article were defrayed in part by the payment of page charges. This article must therefore be hereby marked *advertisement* in accordance with 18 U.S.C. Section 1734 solely to indicate this fact.

Requests for reprints: Raymond V. Fucini, Department of Biology, Sunesis Pharmaceuticals, Inc., 395 Oyster Point Boulevard, South San Francisco, CA 94080. Phone: 650-266-3500; Fax: 650-266-3503. E-mail: fucini@gmail.com

doi:10.1158/1535-7163.MCT-08-0754

drug combinations including Aurora kinase inhibitors and standard chemotherapy agents.

The tumor suppressor gene product p53 has been proposed to play a role in constraining aberrant endoreduplication and a p53-dependent "tetraploidy checkpoint" that arrests tetraploid cells in G_1 has been recently described (27). Such a checkpoint could govern response to Aurora kinase inhibition, with an intact (p53+) checkpoint promoting tetraploidy, and a compromised (p53 null or p53–) checkpoint leading to endoreduplication and eventual apoptosis (28). The data addressing this hypothesis are mixed. For example, in one study, functional p53 status correlated with endoreduplication upon treatment of cells with PHA-739358 (29). Contrary to these results, another study described profound growth inhibition for p53+ PALL-1 and PALL-2 human leukemia cell lines treated with the Aurora inhibitor ZM447439 compared with cells that express mutant p53 alleles (30). It remains unclear whether antiproliferative effects of Aurora inhibition are p53-dependent, or dependent on other factors specific to the cell line being evaluated; therefore, we conducted our investigation using isogenic HCT116 colorectal carcinoma cell lines either expressing intact p53 ($HCT116^{C}$), or depleted for p53 ($HCT116^{p53}$) by RNA interference as a means of assessing the potential role of this pathway in regulating antiproliferative responses to SNS-314 combinations.

In order to select combination and scheduling regimens to test *in vivo*, we first conducted *in vitro* drug combination studies with SNS-314 in combination with common chemotherapeutic agents and found that concurrent administration showed either additive or antagonistic effects, and sequential regimens produced either synergistic or antagonistic activity, depending on p53 status and the order of treatment. Additional scheduling-dependent synergies were observed when SNS-314 was administered in sequence with docetaxel or vincristine. These observations extended *in vivo* as we found that SNS-314 potentiated the antitumor activity of docetaxel.

Both the *in vitro* synergies observed between SNS-314 and agents that target the mitotic spindle and the potentiation seen with docetaxel *in vivo* are consistent with the mechanism of action of an Aurora kinase inhibitor that bypasses the mitotic spindle assembly checkpoint and augments subsequent spindle toxin–mediated mitotic catastrophe and cell death. We refer to this potential phenomenon as "mitotic shock." Our results suggest that SNS-314 will enhance the efficacy of therapies that target the mitotic spindle.

Materials and Methods

Cell Culture

HCT116 SCR and HCT116 p53 RNAi cells were kindly provided by George Stark, Cleveland Clinic, Cleveland, OH. Cells were cultured in DMEM, 10% fetal bovine serum, and 1× antibiotic/antimycotic, and were plated in growth medium in 384-well Falcon plates (BD Biosciences). Cells were seeded in growth medium at a density of 400 to 1,000 cells/well, in 384-well or 96-well plates and allowed to grow overnight at 37°C, 5% CO_2 before compound treatment.

SNS-314 CI_{50} Drug Combination Screen

The cytotoxic panel included the following drugs: gemcitabine and docetaxel were purchased from Toronto Research Chemicals, Inc. 5-FU, 7-ethyl-10-hydroxy-camptothecin (SN-38), vincristine, and daunomycin were purchased from LKT Laboratories, Inc. Nocodazole was purchased from Sigma. Carboplatin was purchased from Henry Schein, Inc. All compounds were serially diluted as a 2-fold series in DMSO with the exception of carboplatin, which was diluted in saline; 11 concentrations were tested per dose-response. Compounds were administered to cells at 10-fold the final concentration in medium. Three concentration ratios of SNS-314 to panel compounds were tested (314/panel): high/high, low/high, and high/low, in which the "high" compound dilution series starts at 10× EC_{50} and "low" dilution series starts at 1× EC_{50}. Single agents were administered at high concentrations. All procedures were done on a Tecan Evo 200 (Tecan Group, Ltd.) robotic platform. Dose schedules were tested by concurrent administration of SNS-314 and single-panel compound, or sequentially with one drug administered for 24 h followed by washout and administration of the second drug for 48 or 120 h.

The combination index (CI), a numerical value that provides a quantitative measure of the extent of drug interaction, is described in Eq. A, in which $C_{A,X}$ and $C_{B,X}$ are the concentrations of drug *A* and drug *B* used in combination to achieve *X*% drug effect, and $IC_{X,A}$ and $IC_{X,B}$ are the concentrations for single agents to achieve the same effect (31). This equation represents the theoretical additive response for two mutually exclusive drugs, and takes into consideration the ratio at which the two compounds are administered. Our assessment of additivity, synergy, or antagonism was based on the Chou-Talalay model for median-effect assessment of drug interactions (32). To avoid distortions in experimental error that can result from transformation of nonlinear data, we determined the CI at EC_{50}, also referred to as the CI at 50% effect, or CI_{50}. EC_{50} values were determined by a four-parameter fit using GraphPad Prism. Four to eight separate experimental CI_{50} values were generated for each combination to determine the mean and 95% confidence interval. Homologous SNS-314 + SNS-314 combinations provided an internal control for additivity and the mean of these data were normalized to $CI_{50} = 1$. Accordingly, heterologous (SNS-314 + cytotoxic) combination values were normalized by this factor. The Mann-Whitney test was applied to determine statistical significance from the additive internal control with $P < 0.05$ deemed statistically significant.

$$CI_{50} = \frac{C_{A50}}{IC_{50A}} + \frac{C_{B50}}{IC_{50B}} \qquad (A)$$

Cell-Based Proliferation Assays

Cell Count. For high-content screening cell count analysis, cells were plated in 384-well black/clear Falcon plates (BD Biosciences). All cells were incubated for a total of 72 h with compound. After the incubation was complete, cell plates were processed for imaging by fixing the cells

in 4% paraformaldehyde and staining with a 1:4,000 dilution of 10 mg/mL Hoechst 33342. All procedures were done on a Tecan robotic platform (Tecan Group). High-content screening images were captured and data analyzed using the Target Activation application, object count per field parameter, on the ArrayScan VTI instrument (Thermo Fisher Scientific Cellomics). Data were normalized to DMSO and no-cell control wells. For mitotic index measurements, cells were plated at 10×10^4 cells/mL in 96-well poly->l-lysine plates, and treated with compound for 16 h, then fixed in 3.7% paraformaldehyde, incubated with a 1:1,000 dilution of MPM-2 primary antibody (PN 05-368, Millipore) and a 1:200 dilution of secondary anti-mouse Alexa Fluor 488 (PN A11001, Invitrogen) and then stained with Hoechst 33342. Images were captured using the ArrayScan HCS (Thermo Fisher Scientific Cellomics) automated fluorescence microscopic imaging system and analyzed using the Cell Cycle BioApplication for quantitation of MPM-2 intensity and DNA content.

Cell Viability Assays. Viability was measured using the CellTiter-Blue cell viability assay (Promega). Cells were treated as described above, although with a 5-day incubation period. Cytotoxicity was determined by measuring intracellular ATP using the CellTiter-Glo Luminescence Cell Viability Assay (Promega). Cells were seeded in white 96-well tissue culture plates (EK-25083, E&K Scientific) at a density of 1,500 to 2,000 cells/well, and a 2× serial dilution of SNS-314 was dosed in combination with fixed concentrations of either docetaxel or vincristine for a total of 72 h. Viability was determined as the ratio between the ATP in treated cells versus control cells. Apoptosis was measured using the caspase-Glo 3/7 system (Promega). Cells were plated in white 96-well plates as described above and treated first with SNS-314 for 24 h, washed with 200 μL of 1× PBS, and fresh medium was added with the second agent for 24 h. All assays were done at least thrice and in accordance with the manufacturer's instructions; experimental values are represented as means ± SD.

Xenograft Studies

Mice (female *nu/nu*) were purchased from Charles River Laboratories and allowed to acclimatize for 3 days from shipping-related stress and their health was assessed daily by observation. Purified water (reverse osmosis) and irradiated food (PicoLab Rodent Diet 20; Dean's Animal Feeds) were provided *ad libitum*, and the animals were kept on a 12-h light and dark cycle. Mice were subcutaneously implanted in the right hind flank with 200 μL of a 2.5 × 10 7 cell/mL suspension (1:1 DPBS with cells/Matrigel). When tumors reached an average volume of 200 mm^3, mice were weighed, randomized by tumor volume ($l \times w \times h \times 0.52$) before initial treatment, assigned ($n = 10$) to the various study groups and treated with vehicle, docetaxel (Taxotere R), SNS-314 or the sequence of the two drugs. For intraperitoneal administration, SNS-314 was formulated in 20% Captisol R and administered at 42.5 mg/kg twice per week for 3 weeks. This was the most efficacious schedule for SNS-314 when administered as a single agent; the maximum tolerated dose for SNS-314 with this schedule of administration was 170 mg/kg with a $T_{1/2}$ of 4.7 h in mouse plasma and 7.5 h in HCT-116 tumor xenografts and a C_{max} of ~100 μmol/L.[3,4] Docetaxel was purchased from Henry Schein, Inc., and was provided as a commercially available injection concentrate (20 mg/0.5 mL). Docetaxel was diluted according to the manufacturer's instructions to 1 mg/mL and injected i.p. at 10 mg/kg twice a week for 3 weeks. This was the maximum tolerated dose for docetaxel with this route and schedule of administration. For the combination groups, the two drugs were administered with a 24-h separation in sequence. The maximum tolerated dose of SNS-314 in combination with docetaxel at this treatment schedule was 42.5 mg/kg biweekly for 3 weeks. Animals were weighed, monitored for signs or symptoms of toxic effects and measured for tumor volumes twice weekly until an end point was met. The end point for each animal in the study was a measured tumor volume >1,200 mm^3 (or 10% of body weight), a greater than 20% body weight loss for two sequential measurements, clinical observations that would be considered moribund (emaciation, dehydration, lack of normal movement, etc.), or severe behavior abnormalities. Tumor growth inhibition was determined by examining the tumor volume graph and calculating the percentage of inhibition relative to the vehicle control group on the last day the control contained at least 75% of the animals. Tumor growth inhibition (TGI) is then calculated with the following equation:

$$\mathrm{TGI} = \frac{(\text{control TV}_x - \text{control TV}_i) - (\text{treatment TV}_x - \text{treatment TV}_i)}{(\text{control TV}_x - \text{control TV}_i)} \times 100 \quad \text{(B)}$$

where TV_x is the average tumor volume on day X and TV_i is the initial average tumor volume. ANOVA was done to calculate statistical significance, defined as $P < 0.05$. All animal experiments were in accordance with protocols approved by the Sunesis Pharmaceuticals, Inc., Institutional Animal Care and Use Committee and in accordance with local state and Federal regulations.

Results

SNS-314 CI Screen

We selected a panel of seven chemotherapeutic drugs to identify combinations that were additive or synergistic with the antiproliferative potential of SNS-314. The drugs surveyed represented a spectrum of mechanisms including DNA strand termination (gemcitabine and 5-FU), DNA intercalation (daunomycin), DNA alkylation (carboplatin), topoisomerase-II inhibition (SN-38), activation of the mitotic spindle assembly checkpoint (docetaxel), and disruption of microtubule dynamics (vincristine). To address the effects of p53 on responses to SNS-314 combinations, we used

[3] Hogan et al. SNS-314, a potent inhibitor of Aurora kinases, shows broad anti-tumor activity and dosing flexibility *in vivo*. International Symposium on Targeted Anticancer Therapies 2007 (TAT 2007).
[4] Evanchik et al. Nonclinical pharmacokinetics, distribution, and excretion of SNS-314, a novel, selective Aurora kinase inhibitor. 2008 European Cancer Conference (ECCO 14).

isogenic HCT116 colorectal cell lines either depleted for p53 protein levels by means of short hairpin RNA interference or the p53-positive parental cell line expressing an short hairpin RNA control (herein referred to as $HCT116^{p53}$ and $HCT116^{c}$, respectively—see Supplementary Fig. S1).[5] SNS-314 combinations were administered under both concurrent and sequential scheduling schemes to determine potential temporal relationships of drug interaction. Lastly, we examined the effect of high and low drug ratios of SNS-314 relative to panel drug (SNS-314/panel ratio is described in Materials and Methods). The antiproliferative effects of drug combinations were measured by a high-content screening cell count proliferation assay and scored with a combination index, a numerical value that provides a quantitative measure of the extent of drug interaction (in this application, the fractional effect is 50%, therefore single agent and combination EC_{50} values were used to calculate a CI_{50}). Our scoring was based on the Chou-Talalay model for median-effect assessment of drug interactions: when $CI_{50} = 1$ drug effects are additive, when $CI_{50} < 1$, less compound is required for a given fractional effect and the combination is synergistic; and when $CI_{50} > 1$, more drug is required and the combination is antagonistic (32). This process is presented in Fig. 1.

CI Screen of SNS-314 with Conventional Anticancer Agents

The CI_{50} analysis of $HCT116^{c}$ and $HCT116^{p53}$ cells with SNS-314 drug combinations is summarized in Table 1. By applying a multivariable approach, we identified condition-dependent outcomes for all SNS-314 combinations tested. Under conditions of concurrent drug exposure when SNS-314 was administered at low concentrations relative to the combined drug (low/high), the responses were additive with the exceptions of carboplatin, which displayed p53-independent antagonism, and vincristine, which acted synergistically to inhibit proliferation in the $HCT116^{p53}$ line. A p53-independent antagonism was observed for all combinations when SNS-314 was administered at a higher ratio (high/low), with the exception of SN-38, which was additive in the $HCT116^{p53}$ line. SNS-314 (high/high) combinations were additive and independent of p53 in the case of carboplatin or gemcitabine, and mixed for daunomycin, being antagonistic in $HCT116^{C}$ but additive in the $HCT116^{p53}$ line. Combination with SN-38 or docetaxel was additive in the $HCT116^{C}$ line but antagonistic in the $HCT116^{p53}$ line. As seen for the (low/high) ratio, administration of vincristine at higher concentrations was synergistic in the $HCT116^{p53}$ line.

In stark contrast to the varied effects seen under concurrent administration, sequential administration of SNS-314 with chemotherapeutic compounds resulted in predominantly additive effects. All combinations tested were additive and independent of p53 status, irrespective of whether SNS-314 was administered first or second in the sequence, or at the same or lower drug ratio. The only exception was gemcitabine, which was synergistic when dosed first in sequence at a high/low ratio in the $HCT116^{p53}$ line. When SNS-314 was administered at a lower drug ratio, with carboplatin first in the sequence, the combination was antagonistic regardless of p53 status. Strong antagonism was seen when 5-FU was administered second in the sequence at a low/high concentrations in $HCT116^{p53}$. Conversely, synergy was seen when vincristine was administered second in the sequence at a low/high ratio in the $HCT116^{c}$ line, a result consistent with the vincristine synergy identified under the low/high concurrent dosing scheme.

Combination of SNS-314 with Spindle Toxins Compromises the Spindle Checkpoint

The cytotoxic activities of microtubule-targeted agents results from a sustained activation of the spindle assembly checkpoint (33). *Vinca* alkaloids (e.g., vincristine, vinblastine, etc.) depolymerize microtubules, preventing the attachment of spindle microtubules to chromosomes and resulting in an inhibition of chromosome alignment during mitosis. Conversely, taxanes (e.g., docetaxel, paclitaxel, etc.) stabilize microtubules and suppress the dynamics of the mitotic spindle which also inhibits chromosome alignment (34). Aurora-B inhibition has been shown to selectively override the spindle assembly checkpoint as activated by taxol, but not by the microtubule-destabilizing agent nocodazole (8, 28). Because vincristine has a mechanism of action similar to that of nocodazole, we investigated whether SNS-314 would override mitotic arrest induced by taxol or vincristine by monitoring MPM-2 reactivity, an established marker of mitosis. As shown in Fig. 2A, concurrent administration of SNS-314 with docetaxel for 16 hours led to a marked 8.2-fold decrease in MPM-2 as compared with a 1.6-fold decrease for coadministration with vincristine. This suggests that a sustained spindle assembly checkpoint could contribute to the synergy observed with vincristine combinations.

It is well-established that cellular exposure to Aurora inhibitors leads to a dramatic increase in nuclear and cellular size as multiple rounds of the cell cycle proceed due to failure of cytokinesis (8). This large cell phenotype often manifests as a cytostatic, rather than cytotoxic response in standard cellular viability assays (35). We examined the effects on cell viability of varying the concentration of SNS-314 in combination with a fixed concentration of docetaxel or vincristine. Compared with a full cytotoxic effect of docetaxel exposure, a lower maximal effect is observed when SNS-314 is administered as monotherapy or concurrently with docetaxel. However, the maximum effect of SNS-314 in combination with vincristine is comparable to vincristine alone (Fig. 2B). Taken together, these data indicated that morphologic and metabolic phenotypes associated with Aurora-B inhibition dominate when SNS-314 is combined with docetaxel, but not with vincristine.

SNS-314 Shows Conditional Synergism with Vincristine and Docetaxel

To better understand the mechanism of the antiproliferative synergy observed for sequential SNS-314 → vincristine

[5] Supplementary material for this article is available at Molecular Cancer Therapeutics Online (http://mct.aacrjournals.org/).

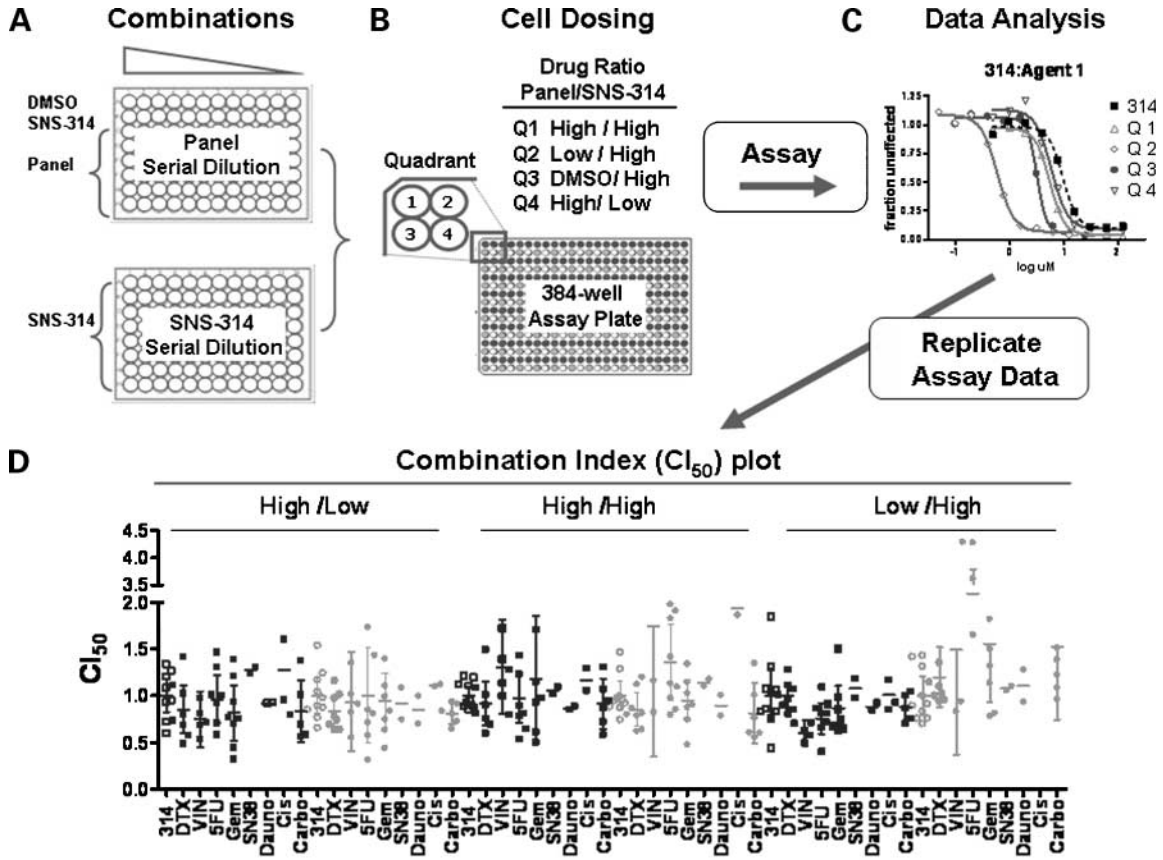

Figure 1. CI_{50} screening process of SNS-314 with cytotoxic anticancer agents. **A,** serial dilution step. Top "panel" plate contains the compound set to be assayed in combination with the test compound (in this application being SNS-314) organized one agent per row, with the exception of DMSO, which serves as an internal control for single-agent SNS-314. Bottom plate contains SNS-314 in all rows. Compounds were serial diluted 2-fold across the plate in DMSO. These plates served as the high ratio concentration samples. Both panel and SNS-314 serial dilution plates were then diluted 10-fold in DMSO to produce two separate low serial dilution plates. **B,** compounds processed in **A** were transferred to a 384-well plate at a 1:1 ratio SNS-314/panel plate. These mixtures were diluted in medium and administered to cells at a 20-fold final assay concentration. **C,** IC_{50} analysis for single-agent and combination dose-response data from **B**. **D,** CI_{50} was calculated from single-agent and combination EC_{50}s using Eq. A for HCT116 cells with wild-type p53 levels (*dark symbols*) or depleted for p53 through RNAi (*light symbols*). Four to eight individual experiments were plotted; the Mann-Whitney test was used to determine statistical significance from internal SNS-314 additive control. Refer to Materials and Methods for more detailed descriptions.

combinations, we examined the morphology of DNA in cells under this administration scheme. Visual analysis by fluorescence microscopy revealed that exposure to SNS-314 for 72 hours caused pronounced endoreduplication with large and multilobed nuclei, as compared with control. Docetaxel caused cells to have either significantly larger nuclei, or evidence of mitotic catastrophe represented as condensed chromatin and fragmented DNA morphologies. Sequential administration of SNS-314 followed by docetaxel increased nuclear size, similar to SNS-314 alone, although with less evidence of fragmented DNA structures. Vincristine-treated cells showed clear evidence of condensed and fragmented DNA (Fig. 3A). These hallmarks of apoptosis-like cell death were also evident in SNS-314-vincristine sequential combination. DNA quantitation supported these observations as SNS-314 → docetaxel–treated cells had increased DNA content, similar to SNS-314 alone, whereas combinations with vincristine had significantly less DNA content (Fig. 3C).

We next measured caspase-3 activity to further examine whether the synergy seen for sequential administration could be attributed, at least in part, to apoptosis. As compared with SNS-314 single agent activity, caspase activity was significantly enhanced when SNS-314 was administered in combination with docetaxel, and this effect was more pronounced in combination with vincristine (Fig. 3B).

A recent report on MK-0457 described time-dependent effects for combinations with docetaxel, in which short-term exposures were additive, whereas long-term exposures resulted in enhanced cell death (36). One possible explanation for these results, and supported by our data, is that drug-induced polyploidy renders cells more susceptible to agents that activate the spindle assembly checkpoint. To further investigate this possibility, we examined whether SNS-314 administration, followed by SNS-314 wash-out (to remove potential for spindle assembly checkpoint bypass) would augment the antiproliferative effects

of prolonged exposure to docetaxel or vincristine. Applying the CI_{50} assessment described earlier, we found that under these conditions, SNS-314 combined with vincristine resulted in strong synergy at both low/high and high/high drug ratios. Synergy was also identified with docetaxel at the high/high ratio, with a clear trend towards synergy at the low/high ratio (Fig. 4). These data are consistent with a mechanism of action in which Aurora inhibition augments the effects of subsequent activation of the spindle assembly checkpoint, resulting in mitotic catastrophe and cell death.

SNS-314 Potentiates Docetaxel Antitumor Activity *In vivo*

Based on the schedule-dependent synergy observed *in vitro*, we examined the effects of SNS-314 in sequential combination with docetaxel on the growth of HCT116

Table 1. Results for SNS-314 CI_{50} drug combination screen conducted in HCT116^{c} or HCT116^{p53} cells under three dosing schedules

Schedule	Cell line	Combination	Ratio (314/panel)											
			High/high				High/low				Low/high			
			Mean	(±) 95% CI	*P*	Result	Mean	(±) 95% CI	*P*	Result	Mean	(±) 95% CI	*P*	Result
(A) Concurrent administration	HCT116c	SNS-314	1.00	0.42		Control	1.00	0.23		Control	1.00	0.29		Control
		Carbo	1.36	0.49	0.562	Additive	1.25	0.26	0.003	Antagonistic	1.78	0.85	0.003	Antagonistic
		GEM	1.41	0.43	0.003	Antagonistic	1.45	0.69	0.023	Antagonistic	0.83	0.49	0.436	Additive
		5-FU	1.25	0.10	0.009	Antagonistic	1.47	0.28	<0.0001	Antagonistic	0.96	0.13	0.853	Additive
		SN38	1.35	0.32	0.076	Additive	1 43	1.44	0.106	Additive	1.06	0.61	0.635	Additive
		Dauno	1.62	0.41	0.008	Antagonistic	1.70	1.06	0.004	Antagonistic	1.04	0.41	0.635	Additive
		DTX	1.21	0.48	0.143	Additive	1.32	0.42	0.005	Antagonistic	1.16	0.31	0.105	Additive
		VIN	1.05	0.21	0.492	Additive	2.13	0.53	0.000	Antagonistic	1.08	0.24	0.492	Additive
	HCT116p53	SNS-314	1.00	0.37		Control	1.00	0.35		Control	1.00	0.56		Control
		Carbo	1.31	0.49	0.056	Additive	1.24	0.76	0.016	Antagonistic	1.70	0.61	0.003	Antagonistic
		GEM	1.37	0.34	0.003	Antagonistic	1.74	0.78	0.001	Antagonistic	0.89	0.63	0.481	Additive
		5-FU	1.33	0.63	0.123	Additive	1.74	1 34	0.004	Antagonistic	0.98	0.62	0.971	Additive
		SN38	1.29	0.75	0.036	Antagonistic	1.63	0.65	0.014	Antagonistic	1.34	0.94	0.142	Additive
		Dauno	1.30	0.93	0.054	Additive	1.76	1 42	0.004	Antagonistic	1.54	1.70	0.076	Additive
		DTX	1.34	0.44	0.043	Antagonistic	1.43	0.58	0.006	Antagonistic	1.02	0.45	0.720	Additive
		VIN	0.76	0.34	0.023	Synergistic	2.56	1.61	0.000	Antagonistic	0.56	0.26	0.005	Synergistic
(B) Sequential SNS-314 ⇨ panel	HCT116p53	SNS-314	1.00	0.20		Control	1.00	0.35		Control	1.00	0.54		Control
		Carbo	0.91	0.54	0.428	Additive	0.84	0.65	0.118	Additive	0.88	0.28	0.562	Additive
		GEM	1.18	1.34	0.965	Additive	0.81	0.60	0.274	Additive	0.86	0.48	0.274	Additive
		5-FU	0.97	0.51	0.573	Additive	0.96	0.51	0.633	Additive	0.76	0.33	0.083	Additive
		DTX	0.92	0.47	0.237	Additive	0.85	0.52	0.237	Additive	1.00	0.26	0.697	Additive
		VIN	1.31	1.01	0.054	Additive	0.75	0.60	0.142	Additive	0.60	0.27	0.024	Synergistic
	HCT116p53	SNS-314	1.00	0.31		Control	1.00	0.37		Control	1.00	0.40		Control
		Carbo	0.81	0.65	0.220	Additive	0.81	0.23	0.118	Additive	1.53	1.57	0.056	Additive
		GEM	0.95	0.44	0.965	Additive	0.95	0.59	0.633	Additive	1.56	1.26	0.068	Additive
		5-FU	1.36	0.82	0.173	Additive	1.00	1.02	0.408	Additive	2.95	1.68	<0.0001	Antagonistic
		DTX	0.86	0.35	0.083	Additive	0.83	0.33	0.122	Additive	1.20	0.64	0.122	Additive
		VIN	1.74	2.78	0.240	Additive	0.94	1.07	0.733	Additive	1.49	2.24	0.188	Additive
(C) Sequential panel ⇨ SNS-314	HCT116c	SNS-314	1.00	0.30		Control	1.00	0.48		Control	1.00	0.26		Control
		Carbo	1.20	0.76	0.108	Additive	0.93	1.12	0.345	Additive	2.10	3.26	0.029	Antagonistic
		GEM	1.20	0.73	0.279	Additive	0.87	0.29	0.235	Additive	0.96	0.77	0.574	Additive
		5-FU	0.95	0.41	0.798	Additive	0.91	0.26	0.442	Additive	1.13	0.97	0.721	Additive
		DTX	1.12	0.47	0.505	Additive	0.86	0.47	0.130	Additive	1.11	0.32	0.279	Additive
		VIN	1.02	2.05	0.933	Additive	1.33	0.88	0.214	Additive	1.08	1.19	1.000	Additive
	HCT116p53	SNS-314	1.00	0.33		Control	1.00	0.26		Control	1.00	0.42		Control
		Carbo	1.33	1.25	0.228	Additive	1.27	2.85	0 755	Additive	2.44	3.26	0.020	Antagonistic
		GEM	1.21	0.72	0.328	Additive	0.71	0.41	0.021	Synergistic	0.98	0.55	0.959	Additive
		5-FU	1.06	0.39	0.798	Additive	0.84	0.45	0.195	Additive	1.65	1.38	0.065	Additive
		DTX	1.13	0.21	0.195	Additive	0.95	0.44	0.505	Additive	1.40	0.70	0.065	Additive
		VIN	1.07	0.67	0.570	Additive	1 21	0.56	0.073	Additive	1.06	0.31	0.808	Additive

NOTE: Deviation for an additive response (where the $CI_{50} = 1$) was scored when the 95% confidence interval was statically distinct from the SNS-314 additive internal control ($P < 0.05$). A $CI_{50} < 1$ was scored as synergistic; $CI_{50} > 1$ was scored as antagonistic.
Abbreviations: Carbo, carboplatin; GEM, gemcitabine; Dauno, daunomycin; DTX, docetaxel; VIN, vincristine; 95% CI, 95% confidence interval.

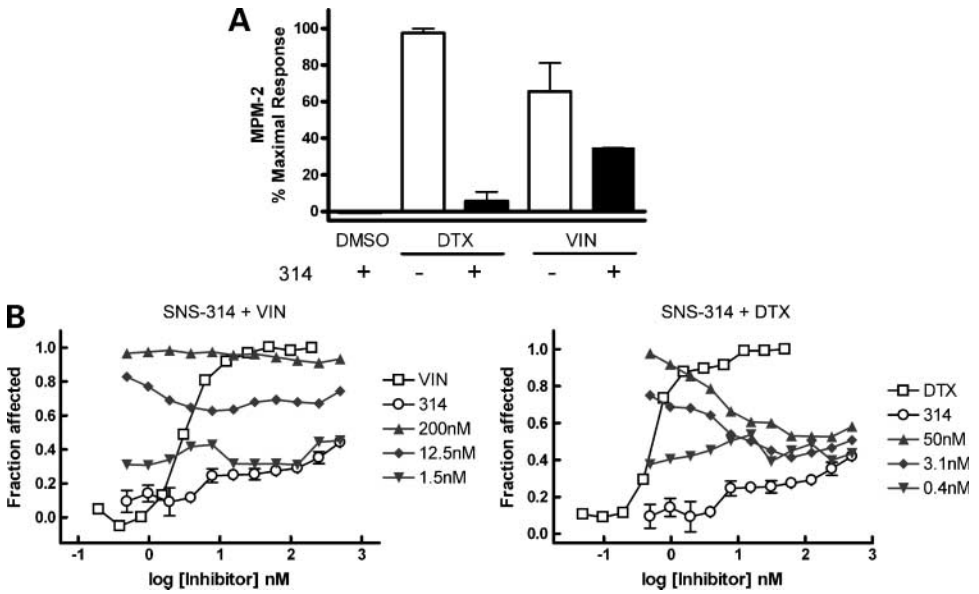

Figure 2. SNS-314 combined with spindle toxins vincristine (*VIN*) or docetaxel (*DTX*) compromises the spindle checkpoint. **A,** MPM-2 staining. Cells were exposed to 13 nmol/L of SNS-314, 12.5 nmol/L of docetaxel, 125 nmol/L of vincristine, 13 nmol/L of SNS-314 + 12.5 nmol/L of docetaxel, or 13 nmol/L of SNS-314 + 125 nmol/L of vincristine for 16 h (drug concentrations approximate SNS-314 IC_{50} and 10-fold excess IC_{50} for docetaxel and vincristine for a low/high combination ratio). MPM-2 staining was determined with the ArrayScan VTI. **B,** varying concentrations of SNS-314 were dosed with fixed concentrations of docetaxel or vincristine for 72 h, and cell viability was measured in a viability assay as described in Materials and Methods.

xenografts. We have previously shown that SNS-314 displays strong antitumor activity and dosing flexibility as a single agent in HCT116 xenograft models.[3] Figure 5 shows the HCT116 tumor growth inhibition after sequential administration of SNS-314 and docetaxel on a biweekly schedule of treatment. Docetaxel was dosed i.p. at 10 mg/kg, which is the maximum tolerated dose in this model when given thrice on a biweekly schedule. Docetaxel could be combined sequentially with 42.5 mg/kg of SNS-314, which represents a 4-fold reduction of the single-agent maximum tolerated dose for SNS-314 when administered i.p. thrice biweekly. These doses and schedules of docetaxel and SNS-314 as single agents did not produce any significant inhibition of HCT116 tumor growth. However, the sequential treatment with SNS-314 followed by docetaxel 24 hours later did produce a significant 72.5% tumor growth inhibition ($P < 0.05$) of HCT116 xenografts. The inverse sequence with docetaxel first followed 24 hours later by SNS-314 mirrored the lack of efficacy observed with the single-agent treatments.

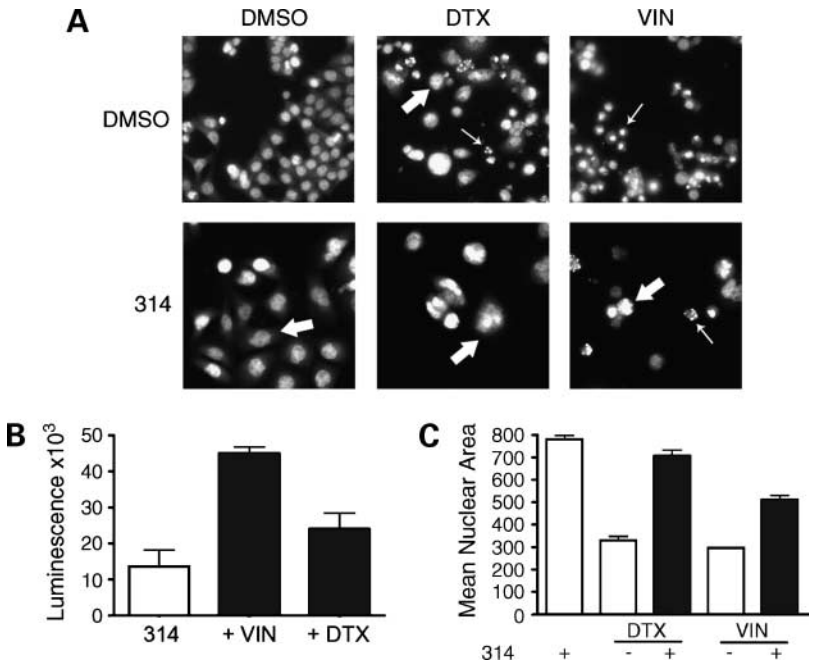

Figure 3. Effects of SNS-314 combinations with docetaxel (*DTX*) or vincristine (*VIN*) under a sequential administration schedule. **A,** representative images of $HCT116^C$ cells administered a sequential combination of SNS-314 plus spindle toxins. Cells were treated with DMSO, 10 nmol/L of docetaxel, 125 nmol/L of vincristine (*top*), or 50 nmol/L of SNS-314, or in combination corresponding to a high/high ration at 125 nmol/L of SNS-314 → 2.5 nmol/L of docetaxel or 125 nmol/L of SNS-314 → 125 nmol/L of vincristine, followed by Hoechst staining. DNA morphologies reveal polyploidy (*large arrows*) and condensed or fragmented chromatin (*thin arrows*). **B,** quantitation of caspase 3 activity was analyzed using a luminogenic substrate as described in Materials and Methods. Cells were exposed to 12 nmol/L of SNS-314, 100 nmol/L of docetaxel, 125 nmol/L of vincristine, 13 nmol/L of SNS-314 + 100 nmol/L of docetaxel, or 12 nmol/L of SNS-314 + 125 nmol/L of vincristine for 16 h (drug concentrations approximate assay IC_{50} for SNS-314 and 10-fold excess IC_{50} for docetaxel and vincristine or a low/high combination ratio). **C,** nuclear area determined by the ArrayScan VTI for combinations as administered in **A**.

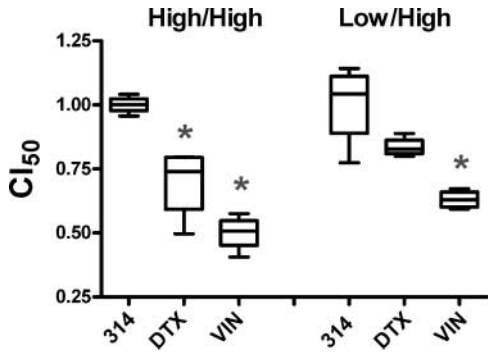

Figure 4. Combination of SNS-314 with spindle toxins results in synergistic inhibition of cell growth. HCT116 cells were dosed sequentially with SNS-314, SNS-314 → docetaxel (*DTX*), or SNS-314 → vincristine (*VIN*). Drug ratio, administration, and CI_{50} determination were conducted as described in Fig. 1, with the exception that the second drug was administered for 120 h (see Materials and Methods).

Significant body weight losses were observed in docetaxel (single agent and combination) treatment groups. Thus, the *in vivo* results parallel those identified *in vitro*.

Discussion

Our previous studies determined that SNS-314 shows potent tumor growth inhibition using an intermittent dose-schedule, a result that supports the potential use of SNS-314 in combination with standard chemotherapeutics. To facilitate the discovery of productive combinations, we applied an automated cell-based screening approach that applies high-throughput screening and high-content screening technologies to evaluate the effects of drug-drug interactions under variable schedules, drug ratios, and p53 conditions. In order to select combination and scheduling regimens to test *in vivo*, we first conducted *in vitro* drug combination studies with SNS-314 in combination with common chemotherapeutic agents including gemcitabine, 5-FU, carboplatin, daunomycin, or SN-38, which function, at least in part, through activation of the DNA damage or mitotic checkpoints. The spindle toxins docetaxel and vincristine are potent spindle assembly checkpoint activators, whereas Aurora B inhibition effectively bypasses the spindle assembly checkpoint under most conditions. Therefore, we examined SNS-314 in combination with microtubule-targeted drugs docetaxel and vincristine, as it has been proposed that activation of the spindle assembly checkpoint followed by its bypass or "slippage" can trigger a massive apoptosis response in cancer cells (37). Our screening results revealed that a concurrent administration at the high SNS-314 ratio resulted in predominantly antagonistic combinations; conversely, we found predominantly additive responses at the low SNS-314 ratio in both wild-type and p53-depleted cells, with the exception of vincristine, which was synergistic. Although further studies are necessary to better understand these responses, they prompted us to investigate scheduling-dependent effects. The sequence of administration had a dramatic effect on response to SNS-314 combinations, as nearly all conditional responses were additive. These data suggest that SNS-314 may be more efficacious when administered under sequential dosing schedules with a common chemotherapeutic.

The proposed p53-dependent postmitotic checkpoint may determine the fate of cells depleted of or inhibited for Aurora activity (27). In one recent study, p53 status-dependent endoreduplication was observed upon treatment of cells with PHA-739358 (29). Another study reported that p53-deficient cell lines were more susceptible to the antiproliferative activities of ZM447439 (7). Conversely, especially profound growth inhibition occurred with the wild-type p53 PALL-1 and PALL-2 human leukemia cell lines after treatment with ZM447439 compared with cells that express mutant p53 (30). Similar relationships have been shown for MK-0457 (VX-680), in which one study reported that cells lacking functional p53 were more susceptible to its antiproliferative activities (28), whereas another study found no relationship between p53 status and sensitivity to this compound or combinations with docetaxel (36). We addressed the issue of p53-dependence directly by conducting this investigation using an isogenic pair of HCT116 colorectal cell lines expressing either with intact p53 or depleted of p53 by RNA interference. Our results mirror these discrepancies reported for p53-mediated effects.

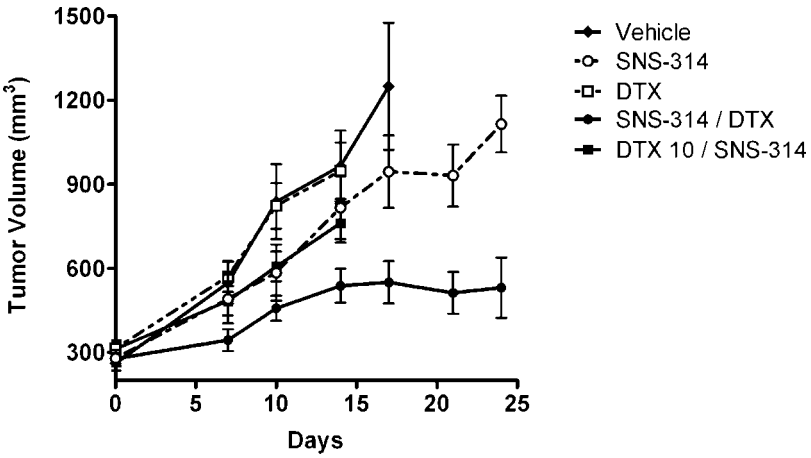

Figure 5. Sequential SNS-314/docetaxel dosing results in significant antitumor activity. Treatment schedules were SNS-314, 42.5 mg/kg biweekly ×3; docetaxel, 10 mg/kg biweekly ×3; SNS-314, 42.5 mg/kg/docetaxel, 10 mg/kg; docetaxel, 10 mg/kg/SNS-314, 42.5 mg/kg. Effects were observed at doses and schedules not efficacious as single agents in HCT116 xenografts. The inverse sequence (docetaxel/SNS-314, 24 h of separation) is not efficacious.

Antagonist combinations were identified when SNS-314 was administered first in sequence with 5-FU in wild-type HCT116 cells or after carboplatin administration regardless of p53 status. Conversely, SNS-314 was synergistic when administered after gemcitabine in p53– cells. Gemcitabine exposure leads to the depletion of cellular dATP pools by inhibition of ribonucleotide reductase and simultaneous disruption of DNA synthesis during S phase, promoting cell accumulation in that phase of the cell cycle. Two hypotheses might account for the synergy resulting from sequential administration of gemcitabine and SNS-314. Depletion of p53 augments premature mitotic entry in gemcitabine-treated cells, so subsequent exposure to SNS-314 may further promote genetic instability. Alternatively, gemcitabine-induced dATP depletion may play a role in augmenting the effects of SNS-314. It is reasonable to suspect that either case would compromise viability. The p53-dependent interactions seen for SNS-314 combinations with DNA-damaging agents carboplatin, 5-FU, and gemcitabine clearly warrant further investigation. However, in this study, we focused on further characterizing the synergy seen for vincristine.

Other recent preclinical studies of Aurora inhibitors have described p53-mediated responses to Aurora inhibition and synergistic interactions with spindle toxins. Yang et al. found that AZD1152 synergistically enhanced the antiproliferative activity of vincristine in acute myeloid leukemia cell line models, both *in vitro* and *in vivo* (38). Sun et al. have described that the Aurora inhibitor BADIM synergized with vinblastine, but not with paclitaxel, to inhibit proliferation of the breast cancer cell line MCF7 (39). Although Hoover et al. reported that MK-0457 (VX-680) was synergistic with docetaxel, they found no p53 context–dependence (36). We have identified a synergistic relationship with concurrent administration of SNS-314 and vincristine in HCT116^{p53}, and in combination with vincristine or docetaxel when the combination was administered in sequence for the parental HCT116^{c} line. These results highlight the potential for SNS-314 combinations to be effective in both p53 positive and negative cancers.

We report here that SNS-314 potentiates the antitumor activity of docetaxel *in vivo*, a result that parallels the synergies observed *in vitro*. Although SNS-314 is an inhibitor of P-gp,[6] it is unlikely that its effects on docetaxel efflux are responsible for the synergy resulting from sequential administration of the two agents. Under our *in vitro* administration scheme, SNS-314 is removed from the medium prior to docetaxel administration. Moreover, it is unlikely that sufficient SNS-314 remains at 24 hours following *in vivo* administration to substantially affect the pharmacokinetics of docetaxel.

Given the importance of Aurora kinases in regulating the spindle checkpoint, it is particularly interesting to find here that combinations with agents which target the mitotic spindle and which depend on the spindle checkpoint for activity, such as paclitaxel, vincristine, and nocodazole (data not shown), increase SNS-314 efficacy. Aurora-B inhibition promotes mitotic slippage resulting in polyploidic cells and genetic instability. Indeed, the extreme nature of polyploidy as induced by Aurora-B inhibitors can result in cellular DNA content ranging from >8N to >32N after 72 hours of exposure (8, 40). This phenomenon likely contributes a variety of cellular stresses that act collectively to ultimately push cells beyond the capacity to maintain viability. Thus, a rapid and aberrant increase in both ploidy and cellular volume could play a role in the antitumor activity seen for Aurora inhibitors *in vivo* and could further render certain cancers susceptible to spindle toxin–induced mitotic catastrophe. A model for which induction of apoptotic or necrotic cell death is dependent on both the activation of the spindle checkpoint and a subsequent slippage from the mitotic arrest has recently been proposed that is consistent with this mechanism of action (37). Taken together, a picture is emerging in which inhibition of Aurora kinase activity may provide a valuable enhancement to these specific chemotherapeutic regimens.

In summary, we have applied a cell-based screening approach to evaluate the effects of SNS-314 interactions with cytotoxic therapeutics. This led to the characterization of sequence-dependent synergistic responses both *in vitro* and *in vivo* for SNS-314 in combination with common chemotherapeutic agents. These data suggest that SNS-314 could have enhanced efficacy when administered sequentially with other standard chemotherapeutic agents. The most profound synergies were identified for agents that activate the spindle assembly checkpoint, e.g., docetaxel and vincristine. These observations were extended *in vivo* using a xenograft model. Taken together, these results highlight the potential for spindle toxins to augment the efficacy of SNS-314. Furthermore, our data suggest that a pan-Aurora inhibitor may increase the antitumor effect of taxanes in malignancies such as colorectal cancer, in which this class of drugs has not been shown to be particularly efficacious. Additional *in vivo* studies are needed to determine whether the modulating effects of SNS-314 on cellular responses observed for docetaxel and vincristine *in vitro* predict responses in the microenvironment of human cancers.

Disclosure of Potential Conflicts of Interest

All authors are current or former employees of Sunesis Pharmaceuticals.

Acknowledgments

We thank Emily Hanan, Andrew Conroy, and Robert McDowell for critical review of this manuscript, and Michelle Arkin for assistance with experimental design.

References

1. Andrews PD. Aurora kinases: shining lights on the therapeutic horizon? Oncogene 2005;24:5005–15.

2. Fu J, Bian M, Jiang Q, Zhang C. Roles of Aurora kinases in mitosis and tumorigenesis. Mol Cancer Res 2007;5:1–10.

3. Vader G, Lens SM. The Aurora kinase family in cell division and cancer. Biochim Biophys Acta 2008;1786:60–72.

[6] P. Taverna. SNS-314, a pan-Aurora kinase inhibitor, shows potent antitumor activity and dosing flexibility *in vivo*. Manuscript in preparation.

4. Kollareddy M, Dzubak P, Zheleva D, Hajduch M. Aurora kinases: structure, functions and their association with cancer. Biomed Pap Med Fac Univ Palacky Olomouc Czech Repub 2008;152:27–33.

5. Katayama H, Sasai K, Kloc M, Brinkley BR, Sen S. Aurora kinase-A regulates kinetochore/chromatin associated microtubule assembly in human cells. Cell Cycle 2008;7:2691–704.

6. Sen S, Katayama H, Sasai K. Functional significance of Aurora kinase A in centrosome amplification and genomic instability. Adv Exp Med Biol 2008;617:99–108.

7. Ditchfield C, Johnson VL, Tighe A, et al. Aurora B couples chromosome alignment with anaphase by targeting BubR1, Mad2, and Cenp-E to kinetochores. J Cell Biol 2003;161:267–80.

8. Hauf S, Cole RW, LaTerra S, et al. The small molecule Hesperadin reveals a role for Aurora B in correcting kinetochore-microtubule attachment and in maintaining the spindle assembly checkpoint. J Cell Biol 2003;161: 281–94.

9. Sasai K, Katayama H, Stenoien DL, et al. Aurora-C kinase is a novel chromosomal passenger protein that can complement Aurora-B kinase function in mitotic cells. Cell Motil Cytoskeleton 2004;59:249–63.

10. Bischoff JR, Anderson L, Zhu Y, et al. A homologue of Drosophila aurora kinase is oncogenic and amplified in human colorectal cancers. EMBO J 1998;17:3052–65.

11. Chieffi P, Cozzolino L, Kisslinger A, et al. Aurora B expression directly correlates with prostate cancer malignancy and influence prostate cell proliferation. Prostate 2006;66:326–33.

12. Fraizer GC, Diaz MF, Lee IL, Grossman HB, Sen S. Aurora-A/STK15/BTAK enhances chromosomal instability in bladder cancer cells. Int J Oncol 2004;25:1631–9.

13. Hu W, Kavanagh JJ, Deaver M, et al. Frequent overexpression of STK15/Aurora-A/BTAK and chromosomal instability in tumorigenic cell cultures derived from human ovarian cancer. Oncol Res 2005;15:49–57.

14. Jeng YM, Peng SY, Lin CY, Hsu HC. Overexpression and amplification of Aurora-A in hepatocellular carcinoma. Clin Cancer Res 2004;10: 2065–71.

15. Katayama H, Brinkley WR, Sen S. The Aurora kinases: role in cell transformation and tumorigenesis. Cancer Metastasis Rev 2003;22: 451–64.

16. Landen CN, Jr., Lin YG, Immaneni A, et al. Overexpression of the centrosomal protein Aurora-A kinase is associated with poor prognosis in epithelial ovarian cancer patients. Clin Cancer Res 2007;13:4098–104.

17. Royce ME, Xia W, Sahin AA, et al. STK15/Aurora-A expression in primary breast tumors is correlated with nuclear grade but not with prognosis. Cancer 2004;100:12–9.

18. Tanaka E, Hashimoto Y, Ito T, et al. The clinical significance of Aurora-A/STK15/BTAK expression in human esophageal squamous cell carcinoma. Clin Cancer Res 2005;11:1827–34.

19. Tchatchou S, Wirtenberger M, Hemminki K, et al. Aurora kinases A and B and familial breast cancer risk. Cancer Lett 2007;247:266–72.

20. Vischioni B, Oudejans JJ, Vos W, Rodriguez JA, Giaccone G. Frequent overexpression of aurora B kinase, a novel drug target, in non-small cell lung carcinoma patients. Mol Cancer Ther 2006;5:2905–13.

21. Carvajal RD, Tse A, Schwartz GK. Aurora kinases: new targets for cancer therapy. Clin Cancer Res 2006;12:6869–75.

22. Gautschi O, Heighway J, Mack PC, Purnell PR, Lara PN, Jr., Gandara DR. Aurora kinases as anticancer drug targets. Clin Cancer Res 2008;14: 1639–48.

23. Girdler F, Gascoigne KE, Eyers PA, et al. Validating Aurora B as an anticancer drug target. J Cell Sci 2006;119:3664–75.

24. Lee EC, Frolov A, Li R, Ayala G, Greenberg NM. Targeting Aurora kinases for the treatment of prostate cancer. Cancer Res 2006;66: 4996–5002.

25. Oslob JD, Romanowski MJ, Allen DA, et al. Discovery of a potent and selective aurora kinase inhibitor. Bioorg Med Chem Lett 2008;18: 4880–4.

26. Robert F, Hurwitz H, Verschraegen CF, et al. Phase 1 trial of SNS-314, a novel selective inhibitor of aurora kinases A, B, and C, in advanced solid tumor patients. J Clin Oncol 26:2008 (May 20 suppl; abstr 14642).

27. Andreassen PR, Lohez OD, Lacroix FB, Margolis RL. Tetraploid state induces p53-dependent arrest of nontransformed mammalian cells in G1. Mol Biol Cell 2001;12:1315–28.

28. Gizatullin F, Yao Y, Kung V, Harding MW, Loda M, Shapiro GI. The Aurora kinase inhibitor VX-680 induces endoreduplication and apoptosis preferentially in cells with compromised p53-dependent postmitotic checkpoint function. Cancer Res 2006;66:7668–77.

29. Carpinelli P, Ceruti R, Giorgini ML, et al. PHA-739358, a potent inhibitor of Aurora kinases with a selective target inhibition profile relevant to cancer. Mol Cancer Ther 2007;6:3158–68.

30. Ikezoe T, Yang J, Nishioka C, et al. A novel treatment strategy targeting Aurora kinases in acute myelogenous leukemia. Mol Cancer Ther 2007;6:1851–7.

31. Zhao L, Wientjes MG, Au JL. Evaluation of combination chemotherapy: integration of nonlinear regression, curve shift, isobologram, and combination index analyses. Clin Cancer Res 2004;10:7994–8004.

32. Chou TC, Talalay P. Quantitative analysis of dose-effect relationships: the combined effects of multiple drugs or enzyme inhibitors. Adv Enzyme Regul 1984;22:27–55.

33. Pasquier E, Kavallaris M. Microtubules: a dynamic target in cancer therapy. IUBMB Life 2008;60:165–70.

34. Jackson JR, Patrick DR, Dar MM, Huang PS. Targeted anti-mitotic therapies: can we improve on tubulin agents? Nat Rev Cancer 2007;7: 107–17.

35. Castedo M, Perfettini JL, Roumier T, Andreau K, Medema R, Kroemer G. Cell death by mitotic catastrophe: a molecular definition. Oncogene 2004;23:2825–37.

36. Hoover RR, Haregewoin A, Harding MW. The Aurora kinase inhibitor MK-0457 (VX-680) demonstrates anticancer activity alone or in combination with docetaxel. Eur J Can Supplements (ECCO 14 Meeting Abstract) 5:2007;6.

37. Tao W, South VJ, Zhang Y, et al. Induction of apoptosis by an inhibitor of the mitotic kinesin KSP requires both activation of the spindle assembly checkpoint and mitotic slippage. Cancer Cell 2005;8:49–59.

38. Yang J, Ikezoe T, Nishioka C, et al. AZD1152, a novel and selective aurora B kinase inhibitor, induces growth arrest, apoptosis, and sensitization for tubulin depolymerizing agent or topoisomerase II inhibitor in human acute leukemia cells *in vitro* and *in vivo*. Blood 2007;110: 2034–40.

39. Sun L, Li D, Dong X, et al. Small-molecule inhibition of Aurora kinases triggers spindle checkpoint-independent apoptosis in cancer cells. Biochem Pharmacol 2008;75:1027–34.

40. Harrington EA, Bebbington D, Moore J, et al. VX-680, a potent and selective small-molecule inhibitor of the Aurora kinases, suppresses tumor growth *in vivo*. Nat Med 2004;10:262–7.

Molecular Cancer Therapeutics

The Aurora kinase inhibitor SNS-314 shows broad therapeutic potential with chemotherapeutics and synergy with microtubule-targeted agents in a colon carcinoma model

Erica C. VanderPorten, Pietro Taverna, Jennifer N. Hogan, et al.

Mol Cancer Ther 2009;8:930-939.